



Mineralogy and Radioactivity of Stream Sediments of Wadi Abu Marw, South Eastern Desert, Egypt

Osama M. Draz, Hani H. Ali and Doaa A. Moustafa

Nuclear Materials Authority, P. O. Box 530, El-Maadi, Cairo, Egypt

Received: 05 Sept. 2023

Accepted: 10 Oct. 2023

Published: 20 Oct. 2023

ABSTRACT

Abu Marw area is situated in the southeastern part of the Eastern Desert, about 120 km South East of Aswan. Geologically, the area is covered by late Proterozoic igneous and metamorphic rocks. These rocks are non-conformably overlain by cretaceous Nubian sandstone. The rocks are arranged from oldest to youngest rocks as follows: metagabbros, metavolcanics, older granites and younger granites. The area is dissected by several wadies e.g. Wadi Abu Marw and dissected by several drainage lines and their tributaries. The available data propose that, the studied stream sediments are potential think for accessory minerals as well as rare metal minerals that may control the geochemical enrichment of trace elements as; Co, Cu, Zn, Zr, Rb, Y, Pb and Nb. The present work adopts the ESEM/EDX –BSE and XRD an appropriate tool for the identification of the accessory minerals. These minerals are categorized as radioactive minerals (uranothorite), radioactive-bearing minerals (monazite and zircon) and non-radioactive minerals (magnetite, ilmenite, leucosene, titanite, jarosite, spessartine, rutile, fluorite, pyrite, apatite, stibiconite, wolframite, hübnerite, scheelite, cuprotungstite meneghinite, bayldonite, cassiterite and bismuth). The radiometric study of the stream sediments of Abu Marw area indicates that the average concentrations of U and Th are 3ppm and 11.59ppm respectively, ranging from 1 to 6ppm for U and 4 to 24ppm for Th, which reveals a significant fractionation during weathering of these sediments.

Keywords: Proterozoic igneous and metamorphic rocks _Wadi Abu Marw_ accessory minerals

Introduction

Abu Marw area is located at the South Eastern Desert of Egypt, and covering an area of about 150 km South East of Aswan. It is entirely covered by igneous and metamorphic rocks that are dissected by several wadies e.g. Wadi Abu Marw and dissected by several drainage lines and their tributaries. The area was studied by many authors, such as El-Afandy (1994), El-Afandy *et al.* (2015) and El-Afandy, and El Shayib (2020) from different point of view. The present study deals with the mineralogy and radioactivity of the stream sediments of Wadi Abu Marw area.

Geologic outlines

The study area is mainly covered by Late Proterozoic igneous and metamorphic rocks. These basement rocks are nonconformably overlain by Cretaceous Nubian sandstone. The cropping rocks of the investigated area are arranged from the oldest to the youngest into: metagabbro, metavolcanics, older granites and younger granites (Fig.1).

The metagabbros constitute a narrow belt exposed along the eastern parts of the studied area. In the southeast part of the studied area the metagabbros have an N-S trend east of Wadi Hadayib, and then it changes to NW direction. Also several isolated masses are observed partly covered by eolian sands in the central part of the studied area. In general, the metagabbros belt present adjacent and parallel to the metavolcanic belt. The contacts between metagabbros and the metavolcanics are structurally contact, but the contacts between the metagabbros and the granitoid rocks are sharp contacts. The metagabbros

Corresponding Author: Osama M. Draz, Nuclear Materials Authority, P. O. Box 530, El-Maadi, Cairo, Egypt

are distinctly layered at the bottom of the masses grading upwards into coarse grained rocks which intern gradually change into fine grained rocks towards the top (El-Afandy 1994).

The metavolcanics are fine to very fine grained rocks and display brown, green and/or grey colors and form low relief mountain ridges. The metavolcanic rocks are intruded by the older granites. The metavolcanics are sometimes capped by Nubian sandstones. These rocks are dissected by many faults mainly striking in ENE-WSW, E-W and NW-SE directions. They are mainly basic to intermediate in composition, but acidic varieties are also present. Metavolcanics are mainly represented by metabasalts, metaandesites, metadacites and metahydacites (El-Afandy,1994).

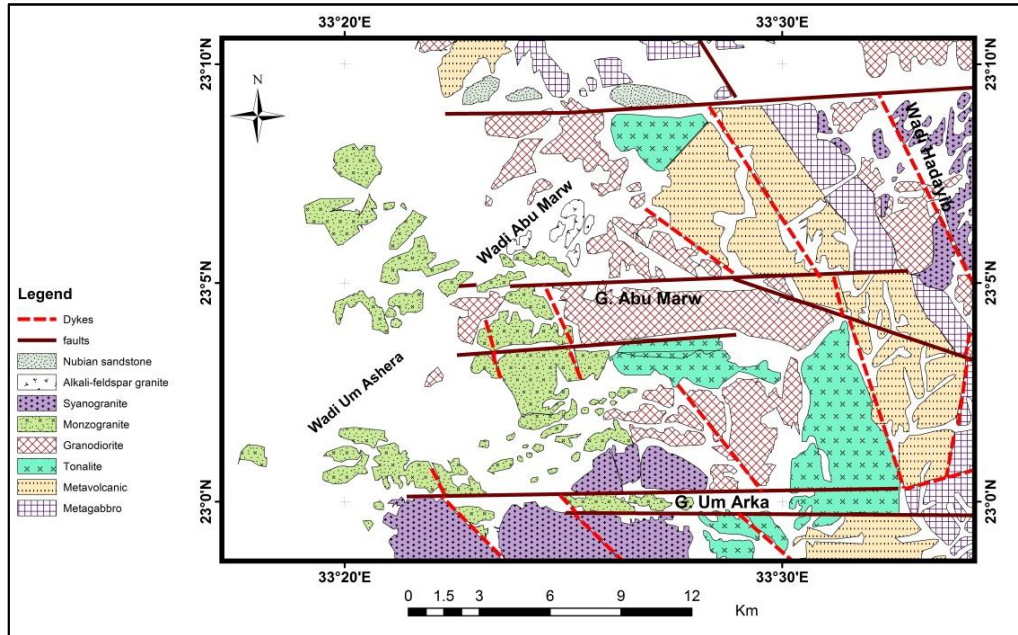


Fig.1: Geologic map of Abu Marw area, South Eastern Desert, Egypt after El- Afandy, 1994.

The granitoid Rocks in the studied area constitute batholithic size bodies which invaded the metavolcanic rocks exposed in the eastern part of the mapped area. The granitoid rocks are partly covered by the Nubian sandstone. Field relations and geological observations revealed that the studied granites are composed mainly of older and younger granites. The older granites are composed of tonalities and granodiorites, while the younger granites are composed of monzogranites, syenogranites and alkali-feldspar granites (El-Afandy, 1994).

The older granites form low relief hill rocks due to their rapid weathering. These rocks are oriented in the ENE-N-S and NW-SE directions. They are characterized by their bouldary appearance, cavernous weathering and exfoliation (Fig.2a). The contacts between the older granites and the surrounding rocks are sharp. These rocks are invaded by a nearly paralleled dykes swarm trending E-W and extending for about 12Km. These dykes are mostly of basic and quartz feldspar porphyry types ranging in width from 3 to10m.

The younger granites are pink to red in color, equigranular and form low to medium topographic terrains (Fig.2b). They have curved linear isolated masses. The contacts between these rocks and the surrounding older rocks are sharp contacts and are dissected by numerous dyke swarms in different direction (Fig.2c). They are highly jointed in different directions, El-Afandy, (1994) (Fig.2d).

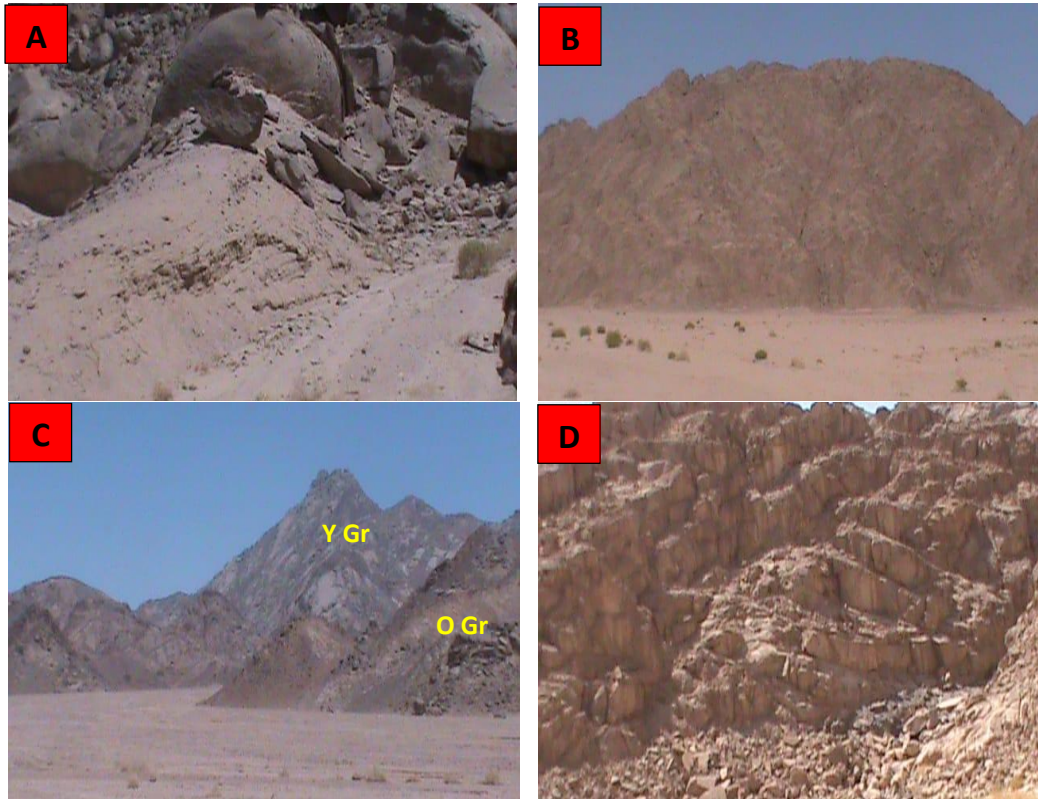


Fig. 2: Photographs showing:
A): Older granites showing exfoliation.
B): Younger granites showing relatively low to medium topography.
C): Basic dyke swarms cut the younger granites.
D): Vertical joints dissecting the younger granites.

Sampling and Methodology

In order to achieve the main goal of this study, several applications were used. A total of 22 stream sediment samples were collected from W. Abu Marw area (Fig. 3) through an open pit samples of 50 cm diameter and depth of one meter, the sample spacing were 500 m apart and the average weight of each samples is about 5 kg.

The collected stream sediments samples were quartered and the representative samples were put in a cylindrical plastic container (9.5 cm in diameter and 3 cm high) which contained about 300 gm of the sample for the radiometric analyses. The containers were well sealed and left for 28 days to accumulate free radon and attain radioactive equilibrium. The instrument used consists of a bicorner-scintillation detector from NaI (TI). In this technique, four energy regions of interest representing ^{234}Th , ^{212}Pb , ^{214}Pb and ^{40}K isotopes are used to estimate eU, eTh, Ra and K, respectively.

For quantitative mineralogical analyses, the collected samples were dried and sieved using 2mm sieve to discard gravel fractions and the rest of samples were quartered using John's Splitter and an automatic rotary splitter to obtain representative samples (about 60-80gm) for different mineralogical treatments. Each sample was sieved to get three fractions; ($<800\mu\text{m}$, $800\mu\text{m}-63\mu\text{m}$ and $>63\mu\text{m}$). The size fraction ranging between $800\mu\text{m}-63\mu\text{m}$ for each sample subjected to decantation method to remove silt and clay particles. Quantitative mineralogical analyses for the stream sediment samples were carried out by heavy liquid separation using bromoform solution (sp. gr. 2.86 g/cm^3) then the magnetite of each sample was collected by hand magnet and the magnetite free samples were subjected to magnetic fractionation using a Frantz Isodynamic Magnetic Separator (Model L-1). The condition characterized Frantz Isodynamic Magnetic Separator at side slope of 5° , forward slope of 20° and step of currents 0.2, 0.5, 1.0, 1.5 magnetic and 1.5 non-magnetic current amperes.

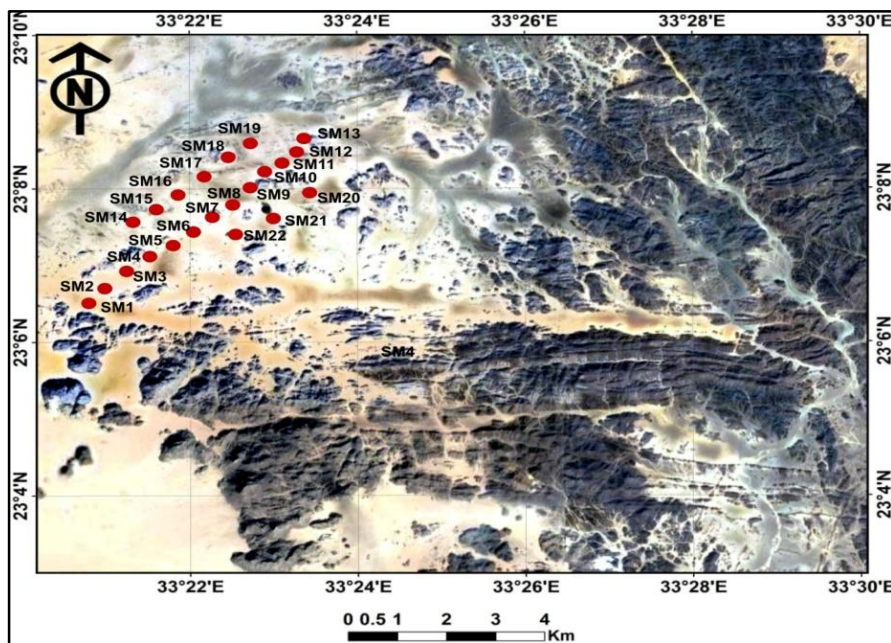


Fig. 3: Google earth image shows the location of collected samples from W. Abu Marw area.

Mineralogical investigation of the mineral constituents of the stream sediments of Wadi Abu Marw was carried out by X-ray diffraction technique. Phillips X-ray diffraction (Model PW-1010) with a scintillation counter (MODEL pw-25623/00) and Ni filter was used. Semiquantitative EDX chemical analyses were carried out using a Phillips XL-30 Environment Scanning Electron Microscope (ESEM). Additionally, the geochemical study was done (trace elements) on the stream sediments using PHILIPS X' Unique-II spectrometer with automatic sample changer PW 1510, (30 positions). All analyses were achieved in the Central Labs of the Nuclear Materials Authority (NMA).

Mineralogy

The heavy minerals recognized microscopically are categorized to radioactive minerals (uranthorite), radioactive-bearing minerals (monazite and zircon) and non-radioactive minerals (magnetite, ilmenite, leucoxene, titanite, jarosite, spessartine, rutile, fluorite, pyrite, apatite, stibiconite, wolframite, hübnerite, scheelite, cuprotungstite meneghinite, bayldonite, cassiterite and bismuth) as well as the green silicates. In the following paragraphs, the detected minerals will be displayed and described in some details.

Uranthorite [(Th,U)SiO₄] is the most abundant uranium and thorium mineral which is a variety of thorite minerals rich in uranium. It is isomorphous with zircon and strongly radioactive (Fron del, 1958). In the studied samples, uranthorite occur as subhedral to anhedral grains ranging in color from yellowish brown to brown with vitreous and resinous luster (Fig. 4A). The brownish tint of the studied grains may be due to the incrustation with iron oxides (El- Nahas, 2006). The EDX microanalysis data indicate the presence of Th (48.85%), U (11.95%), Y (11.67 %), Si (9.73%), Fe (4.15%) and Zr (3.2%). The presence of Y may attribute to inclusion of xenotime as solid solution within uranthorite.

Monazite [(Ce,La,Th,Nd)PO₄] is one of the most important nuclear minerals, being a major host for REEs and actinides Th and U (Hinton and Paterson 1994, Bea *et al.*, 1994& Bea 1996). It is widely disseminated in granitic rocks and schistose metamorphic rocks as well as the detrital sediments and typically associated with zircon and sphene. The separated grains occur as rounded to oval form ranging in color from colorless to pale yellow with vitreous luster (Fig. 4B). The EDX microanalysis data indicate the presence of Ce (27.55%), La (15.18%), Nd (10.92%), Pr (3.74%), Sm (2.45%), Gd (1.67%), Th (6.24%) and P (21.67%).

Zircon ($ZrSiO_4$) is a common accessory mineral present in the igneous rocks, particularly in the plutonic rocks and especially those rich in sodium (Deer *et al.*, 1992). Zircon is a significant host for REE, Th and U (Finch and Hanchar, 2003). In the present study, it is relatively abundant exhibits wide variety in color and morphology. The studied zircon grains have euhedral to subhedral form. They are mostly long prismatic grains, while some crystals are short and have good adamantine luster. Elongation is seen in some of the zircon grains examined indicating a significant fluid content in the magma and validating the magmatic origin (Pupin *et al.*, 1978; Dardier, 1999; El Mansi *et al.*, 2004; Omran and Dessouky 2016). The most of the prismatic zircon grains are characterized by bipyramidal terminations. The recorded zircon has yellow, yellowish red to reddish brown colors and sometimes has colorless to pale yellow colors (Fig. 4C). The majority of zircon grains are transparent and rarely translucent. The EDX microanalysis data indicate the presence of Zr (6.63%), Th (42.16%), U (15.96%), Y (6.75%) and Si (15.81%).

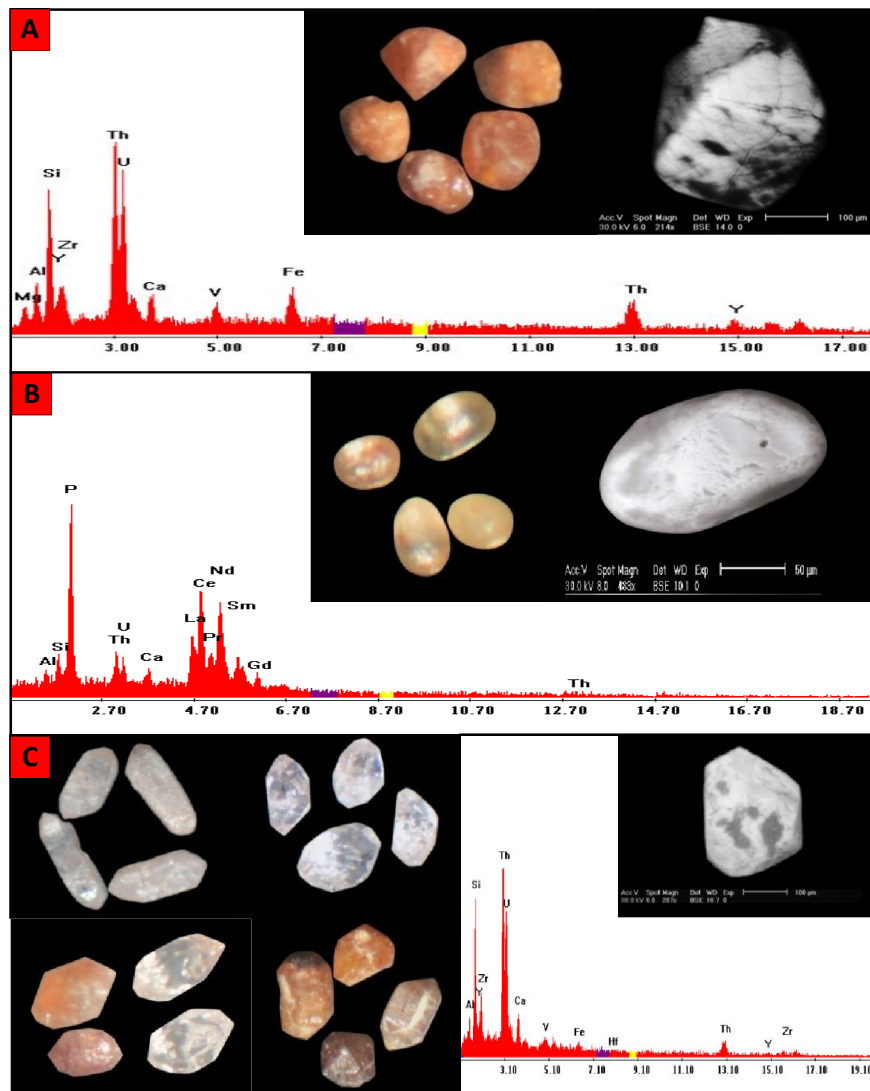


Fig. 4: (A) Photomicrograph of uranothorite grains, EDX pattern and BSE image.
(B) Photomicrograph of monazite grains, EDX pattern and BSE image.
(C) Photomicrograph of different zircon grains, EDX pattern and BSE image.

The presence of Th, U and may reflect the presence of uranothorite while the presence of Y may reflect the presence of xenotime. Förster (2006) reported the presence of intermediate solid solutions in the Th-Y-Zr-U system in evolved and metasomatically altered P-poor leucogranites of either I- or A-type

affinity. Solid solutions with different ranges could be resulted between these minerals and produced zirconian thorite, thorian zircon, yttrian zircon and yttrian thorite. El Aassy *et al.*, (2006a) stated that zircon of Wadi Ghadir, south Sinai, Egypt is partly dissolved in the presence of Th and U-rich hydrothermal solution and ultimately forms thorite and uranothorite.

Magnetite (Fe_3O_4) is predominant and represents the major part of opaque grains of the studied samples. Magnetite displays black to deep reddish brown color, with metallic to dull luster. Their habit ranges from massive, granular, angular to sub-angular and the octahedron crystals of magnetite are less frequent and occur as isolated grains (Fig. 5A). The EDX microanalysis data indicate the presence of Fe (73.7%) and O (26.3%).

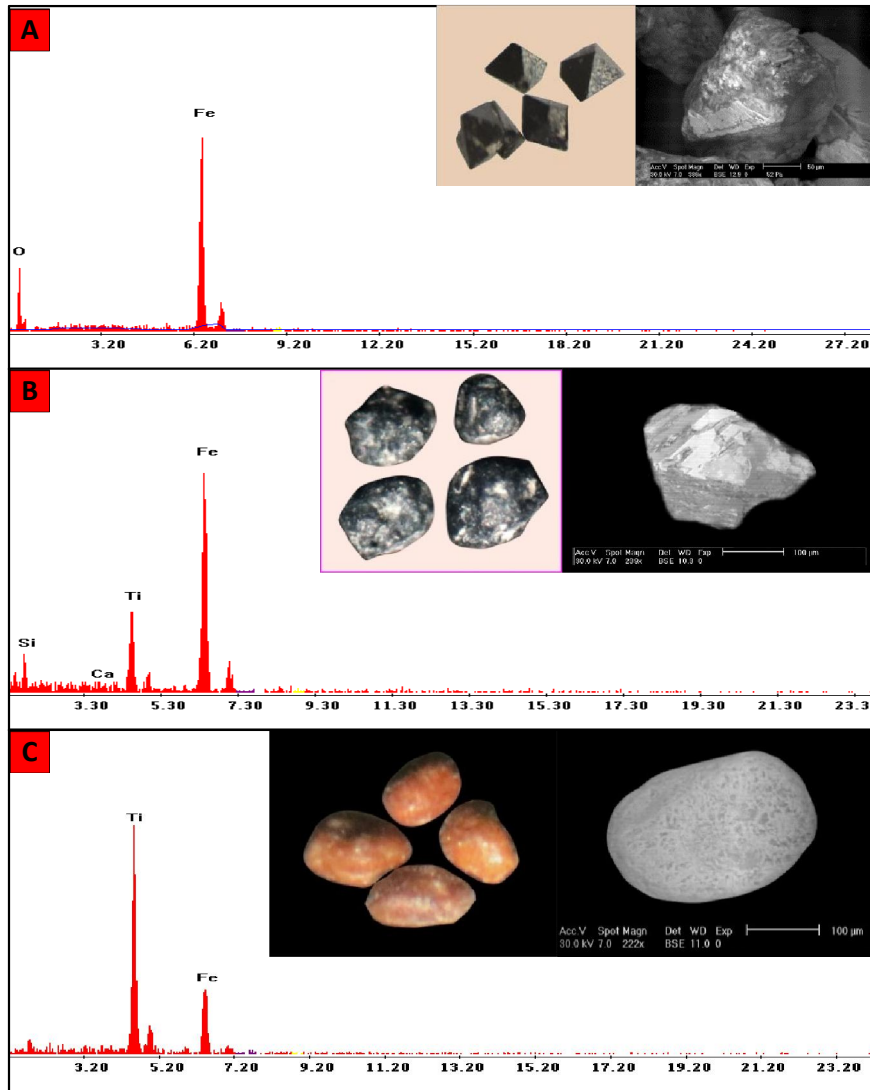


Fig. 5: (A) Photomicrograph of magnetite grains, EDX pattern and BSE image.
(B) Photomicrograph of ilmenite grains, EDX pattern and BSE image.
(C) Photomicrograph of leucoxene grains, EDX pattern and BSE image.

Ilmenite (FeTiO_3) is the most abundant Fe-Ti oxide mineral that occur in a wide variety of igneous rocks, some metamorphic rocks, and as detritus mineral grains. It exhibits iron-black color with metallic luster and occurs as massive, granular, nearly rounded and subrounded grains (Fig. 5B) some grains exist with brownish black color which reflects the partial alteration of these grains. The EDX

microanalysis data show that ilmenite mineral composed mainly of Fe (74.29%) and Ti (15.43%) with minor amount of Si and Ca.

Leucoxene (mixture of Fe-Ti oxides) is not a mineral but it represents the transitional phase during the alteration of ilmenite to form the secondary rutile (Mohamed, 1987, Mohamed, 1998 and Elsner, 2010). It displays rounded to subrounded grains with smooth or pitted surface ranging in color from yellow to yellowish brown and dark brown (Fig. 5C). The EDX microanalysis data show that ilmenite mineral composed mainly of Fe (39.63%) and Ti (60.37%).

Titanite (CaTiSiO_5) is wide spreading in acidic, intermediate igneous rocks and in several metamorphic rocks as accessory phase. Titanite is the abundant accessory mineral in the studied stream sediments; it occurs as subhedral to euhedral grains of adamantine luster and imperfect cleavage exhibiting transparent to translucent yellow to yellowish brown color (Fig. 6A). EDX microanalysis data indicate the presence of Ca (30.72%), Ti (32.71%) and Si (29.02%) with minor amount of Fe and Al. The X-ray diffraction diffractogram in figure (6B) shows that the picked titanite grains are matching with the ASTM card No. (11-142).

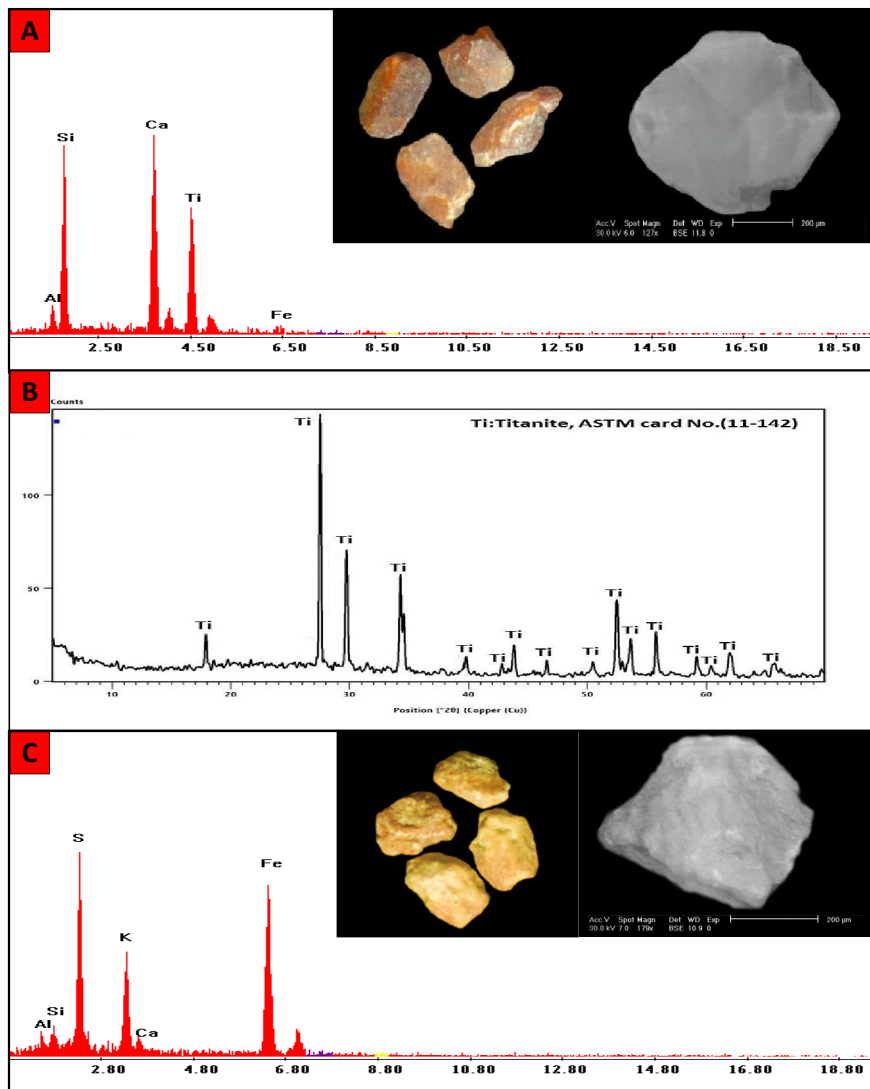


Fig. 6: (A) Photomicrograph of titanite grains, EDX pattern and BSE image.
(B) X-ray diffraction pattern of titanite mineral.
(C) Photomicrograph of jarosite grains, EDX pattern and BSE image.

Jarosite $[K Fe_3 (SO_4)_2 (OH)_6]$ is formed as ore deposits by the oxidation of iron sulfides and commonly associated with acid mine drainage and acid sulfate soil environments. The separated grains of jarosite occur as massive to granular form ranging in color from dark yellow to yellowish brown with vitreous to dull luster (Fig. 6C). The EDX microanalysis data indicate the presence of Fe (49.44%), S (26.14%) and K (15.81) with minor amount of Si, Al and Ca.

Spessartine $[Mn_3Al_2 (SiO_4)_3]$ Garnet is generally considered as characteristic mineral of metamorphic rocks as well as being found in some granites and pegmatites and acid volcanic rocks (Deer *et al.*, 1992). Garnets in metamorphosed manganese bearing assemblages commonly contain spessartine as a principal component in solid solution. In the present study, the spessartine occurs as euhedral to subhedral grains exhibiting red orange color with vitreous luster (Fig. 7A). The EDX microanalysis data show that, spessartine have Si (48.86%), Al (25.69%), Mn(14.3%) and Fe (8.25%) which indicate that spessartine and almandine exist as solid solution. The X-ray diffraction diffractogram in figure (7B) shows that the picked spessartine grains are matching with the ASTM card No. (01-089-4376).

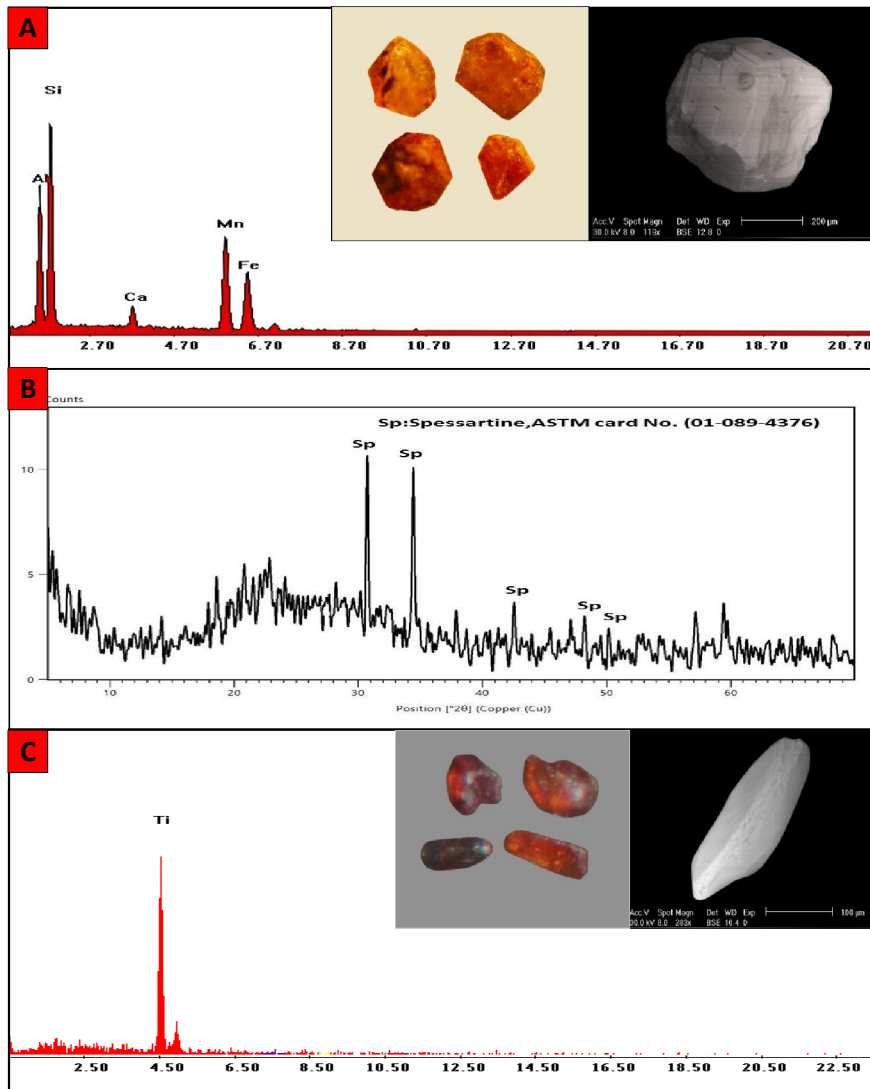


Fig. 7: (A) Photomicrograph of spessartine grains, EDX pattern and BSE image.
(B) X-ray diffraction pattern of spessartine mineral.
(C) Photomicrograph of rutile grains, EDX pattern and BSE image.

Rutile (TiO₂) is the preferred mineral for the production of titanium dioxide and occurs as an accessory mineral in many types of igneous rocks, some metamorphic rocks under high pressure and temperature conditions and as detrital mineral grains. Rutile mineral grains occur as tabular, prismatic and sometimes chevron (elbow) grains exhibiting deep red color with adamantine luster (Fig. 7C). The EDX microanalysis data indicate that, the rutile mineral contains Ti (100%).

Fluorite (CaF₂) occurs in different geological environments particularly in granites and pegmatites, and it has close geochemical association with U, Th and REE. It is always recorded in the radioactive samples of the different rock units under consideration. Khazback and Raslan (1995); Sherif (1998) and Bishr (2007) remarked a positive relation between color of fluorite and the accompanying uranium minerals or to the presence of Y in particular (Fayziev, 1990). The granites enriched in uranium minerals usually contain fluorite crystals of blue, violet and deep violet or even black. The separated fluorite grains occur as massive form ranging in color from colorless to deep violet with vitreous luster (Fig. 8A). The EDX microanalysis data of fluorite reveals that it is composed of Ca (58.07%) and F (41.93%). The X-ray diffraction analysis detected the presence of fluorite mineral associated with quartz and wolframite and matching the ASTM card No. (4-864) (Fig. 10B).

Pyrite (FeS₂) is the most common of the sulfide minerals usually found associated with other sulfides or oxides in quartz veins, sedimentary rocks, igneous rocks and metamorphic rocks. The separated grains of pyrite occur as cubic to massive crystals ranging in color from pale brass yellow to brass yellow with metallic luster (Fig. 8B). The EDX microanalysis data show that cubic pyrite contains Fe (32.61%) and S (67.39%).

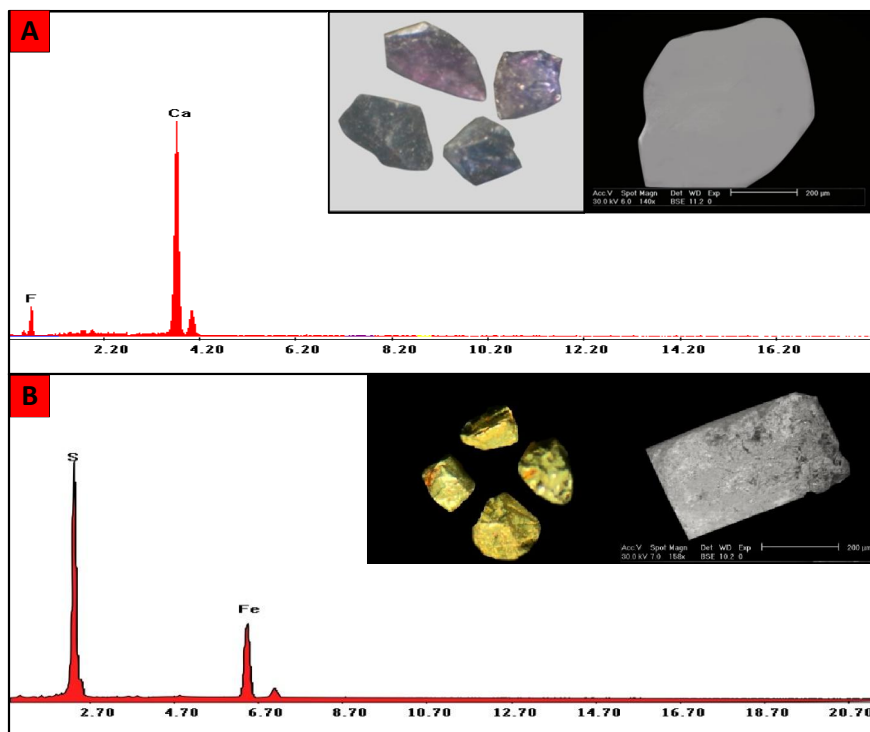


Fig. 8: (A) Photomicrograph of fluorite grains, EDX pattern and BSE image.
(B) Photomicrograph of pyrite grains, EDX pattern and BSE image.

Apatite [Ca₅(PO₄)₃F] is one of few minerals that are produced and used by biological micro-environmental systems. It is the most common phosphate mineral and is the main source of the phosphorus required by plants. It occurs as subrounded to oval grains exhibiting yellowish white, pale yellow and pale brown color (Fig. 9A). The roundness and the pitted surface of apatite grains suggest its transportation. The EDX microanalysis data indicate the presence of Ca (59.86%) and P (28.59%) with minor amount of Si, Al and Fe.

Stibiconite [Sb₃O₆(OH)] is a secondary mineral in hydrothermal mineral deposits, formed by the oxidation of other antimony-bearing minerals, commonly stibnite, which it may entirely replace. In the present study, stibiconite occurs as unihedral grains exhibiting pale yellow to yellowish white and brownish to yellowish red with earthy luster (Fig. 9B). The EDX microanalysis data indicate the presence of Sb (66.1%), Cu (18.58%) Pb (8.44%) Fe (3.27%) and Si (3.61%). The X-ray diffraction diffractogram in figure (9C) shows that the picked stibiconite grains are matching with the ASTM card No. (74-0130) associating with pyrochlore [(Pb₂(Ti Sb)O_{6.5}] and conicalcite [2CaO.2CuO.As₂O₅.H₂O] minerals with the ASTM cards No. (1-078-1547) and (11-307) respectively.

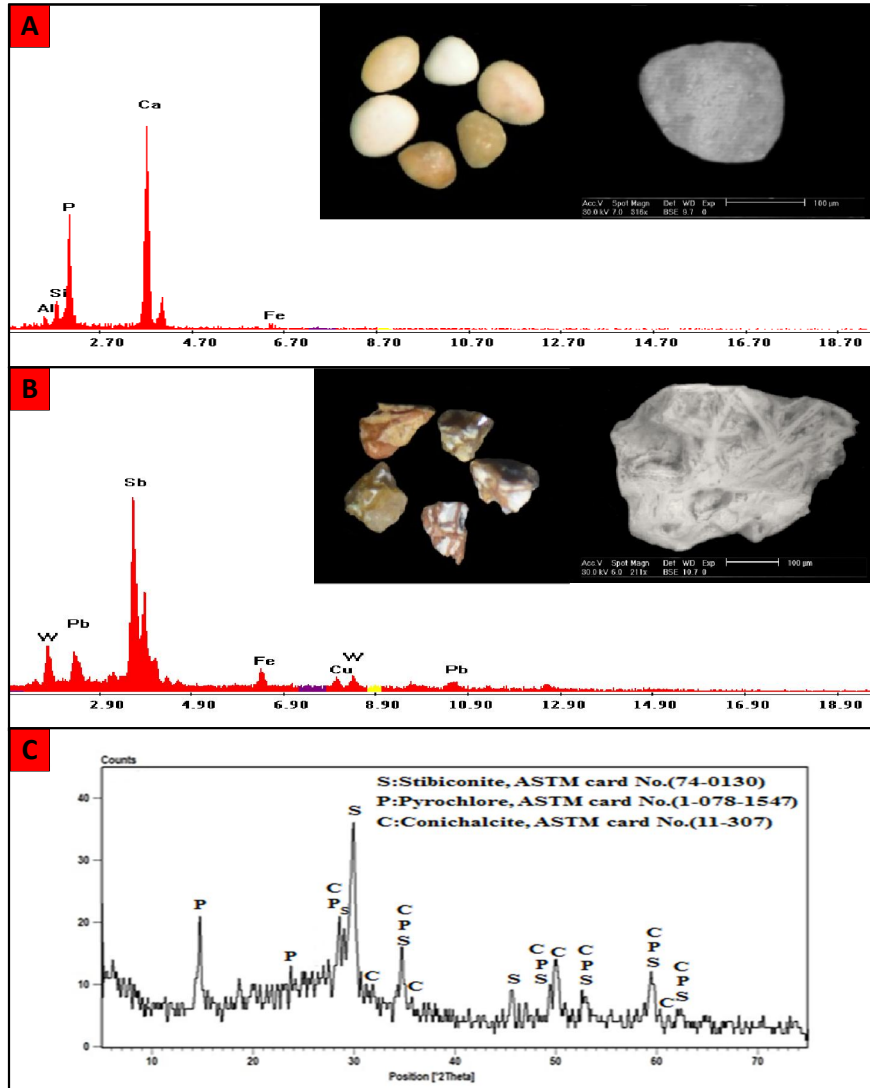


Fig. 9: (A) Photomicrograph of apatite grains, EDX pattern and BSE image.
(B) Photomicrograph of stibiconite grains, EDX pattern and BSE image.
(C) X-ray diffraction pattern of stibiconite mineral.

Wolframite (FeMnWO₄) Hubnerite or (Hübnerite) (MnWO₄) and Scheelite (CaWO₄): In general, tungsten-bearing ores are generally classified in two mineral groups: the wolframite and scheelite groups. In the first, wolframite [(Fe, Mn)WO₄] includes the solid solution series between ferberite (FeWO₄) and hubnerite (MnWO₄) (Horsnail 1979; Sengupta *et al.*, 1987; Gbaruko and Igwe 2007; McClenaghan *et al.*, 2014; Srivastava *et al.*, 2019). The second group, scheelite (CaWO₄) itself is the only commercially important member of the scheelite group (Martins 2014). They are the principal and primary ore minerals of tungsten which found in quartz veins and pegmatites associated with granitic

intrusions, high temperature hydrothermal vein deposits, altered granites with greisen and in alluvial deposits (Goldmann *et al.*, 2013; Harzanagh *et al.*, 2017). In the present study, wolframite occurs as unihedral grains exhibiting grayish to brownish black color with submetallic luster (Fig. 10A). The EDX microanalysis data indicate the presence of W (69.91%), Mn (23.7%) and Fe (1.61%). The X-ray diffraction diffractogram in figure (10B) shows that the picked wolframite grains are matching with the ASTM card No. (11-591) associating with quartz and fluorite. Hubnerite occurs as subhedral to euhedral tabular crystals exhibiting reddish brown to brownish black color with metallic to adamantine luster (Fig. 10C). The EDX microanalysis data indicate the presence of W (79.86%) and Mn (20.14%). Scheelite occurs as irregular massive grains exhibiting yellowish brown, reddish brown and brown color with vitreous to adamantine luster (Fig. 10D). The EDX microanalysis data indicate the presence of W (77.38%) and Ca (20.81%).

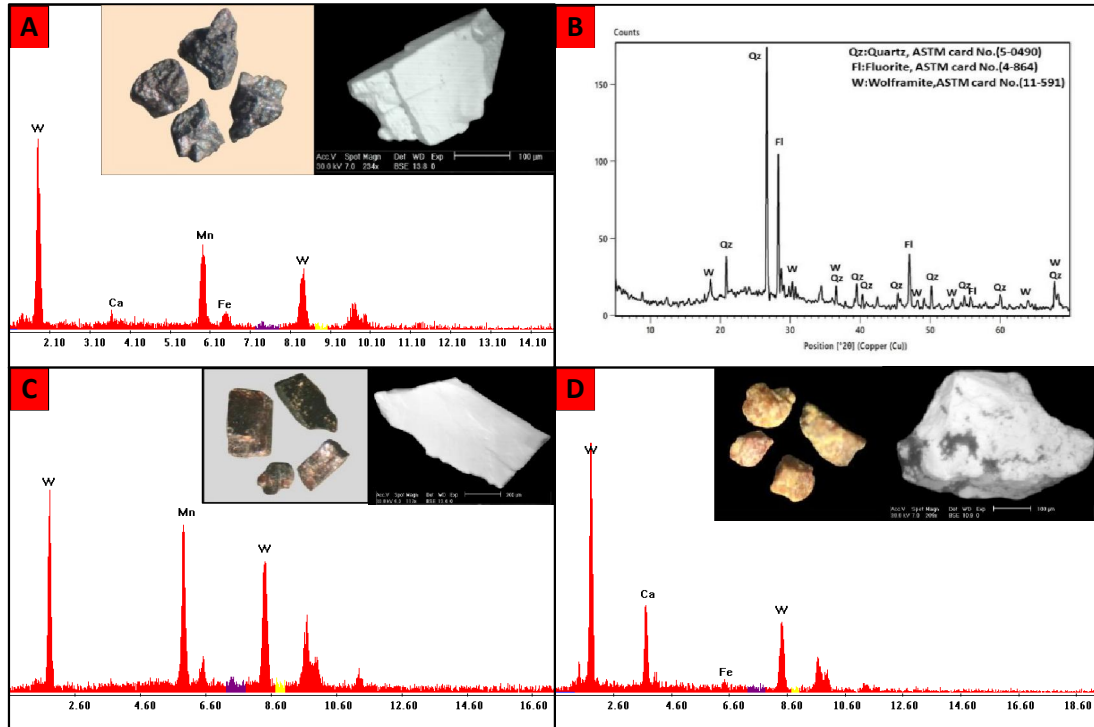


Fig. 10: (A) Photomicrograph of wolframite grains, EDX pattern and BSE image.
(B) X-ray diffraction pattern of wolframite mineral.
(C) Photomicrograph of hubnerite grains, EDX pattern and BSE image.
(D) Photomicrograph of scheelite grains, EDX pattern and BSE image.

Meneghinite ($\text{CuPb}_{13}\text{Sb}_7\text{S}_{24}$) is uncommon mineral but widespread in hydrothermal veins, also contact metasomatic and volcanogenic sulfide deposits. In the present study, it occurs as massive unihedral to tabular grains exhibiting blackish lead-gray color with metallic luster (Fig. 11A). The EDX microanalysis data indicates the presence of Cu (40%), Pb (17.5%) Sb (18.42%), S (13.09%) and Ag (6.1%). The X-ray diffraction diffractogram in figure (11B) shows that the picked meneghinite grains are matching with the ASTM card No. (8-7).

Bayldonite [$\text{PbCu}_3(\text{AsO}_4)_2(\text{OH})$] is a secondary mineral in the oxidized zone of some polymetallic deposits. In the studied area, it occurs as unihedral grains exhibiting apple-green color with resinous luster (Fig. 11C). The EDX microanalysis data indicate the presence of Pb (64.66%), Cu (24.22%) and As (9.55%). The X-ray diffraction diffractogram in figure (11D) shows that the picked bayldonite grains are matching with the ASTM card No. (6-0335).

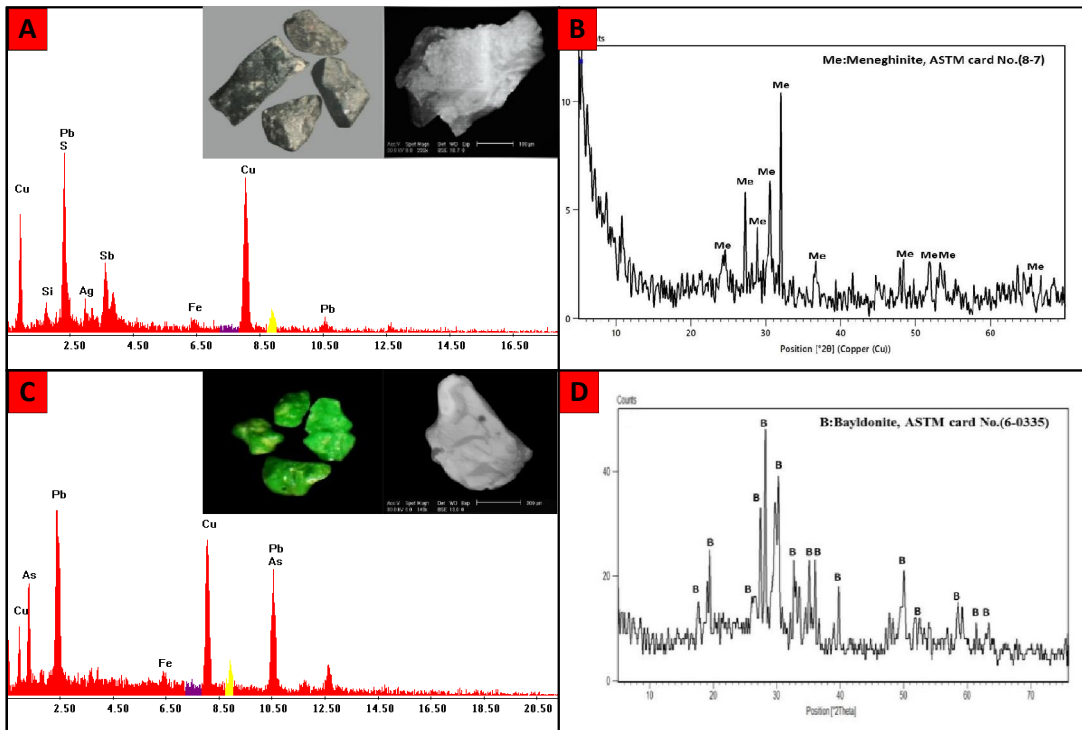


Fig. 11: (A) Photomicrograph of meneghinite grains, EDX pattern and BSE image.
(B) X-ray diffraction pattern of meneghinite mineral.
(C) Photomicrograph of bayldonite grains, EDX pattern and BSE image.
(D) X-ray diffraction pattern of bayldonite mineral.

Cuprotungstite $[\text{Cu}_2(\text{WO}_4)(\text{OH})_2]$ is a rare secondary mineral commonly occurring as the result of scheelite altering in copper-rich environment. In the present study, it occurs as unihedral grains exhibiting emerald green color with vitreous luster (Fig. 12A). The EDX microanalysis data indicate the presence of W (64.73%) and Cu (33.65%).

Cassiterite (SnO_2) is the primary ore of tin and found in hydrothermal veins and pegmatites associated with granite intrusions as well as concentrated in alluvial placer deposits. In the present study, it occurs as massive to subrounded grains exhibiting dark reddish brown color with adamantine luster (Fig. 12B). The EDX microanalysis data revealed that, cassiterite is mainly composed of Sn (100%).

Bismuth [Bi] is relatively rare in Abu Marw stream sediments. It is of creamy white color. Read (1970) stated that, bismuth ores occur in nature in three main associations with tin and copper minerals as in the Bolivian deposits, cobalt as at Schoenberg, Saxony and gold as in the Australian deposits. The EDX microanalysis data (Fig. 12C) indicate the presence of Bi (45.41).

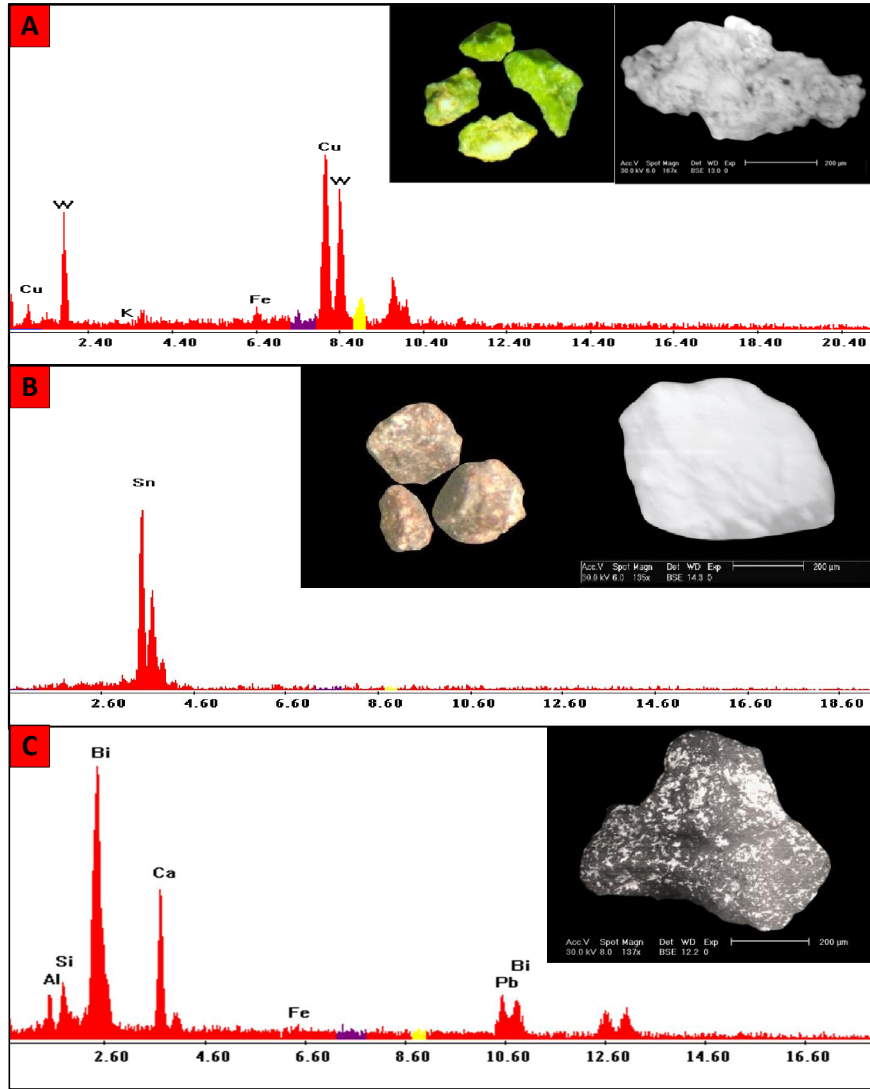


Fig. 12: (A) Photomicrograph of cuprotungstite grains, EDX pattern and BSE image.
(B) Photomicrograph of cassiterite grains, EDX pattern and BSE image.
(C) EDX pattern and BSE image of bismuth mineral.

Geochemistry of Trace Elements

Trace elements concentrations in the stream sediments resulted from the competing influences of provenance, weathering, diagenesis, sediment sorting and the aqueous geochemistry of the individual elements (Rollinson, 1993).

The geochemical analyses of 22 stream sediments of Wadi Abu Marw were analyzed for Cr, Co, Ni, Cu, Zn, Zr, Rb, Y, Ba, Pb, Sr, V and Nb and the results are listed in (Table 1) and the average concentrations compared with UCC are illustrated in figure (12).

From the obtained results, it can be concluded that, these stream sediments are slightly enriched in Co, Cu, Zn, Zr, Rb, Y, Pb and Nb compared with Upper Continental Crust (UCC), Rudnick and Gao, (2003), and depleted in Cr, Ni, Ba, Sr and V. High Zr contents (av. 244.18 ppm), which is higher than the UCC (193 ppm) is attributed to the abundance of zircon in the stream sediments. Cu and Zn are also enriched (554.68 and 75.95 ppm respectively), which are higher than the UCC (28 and 67 ppm), this may reflect the contribution of some basic rocks in the source of the studied stream sediments. Rb content is enriched (av. 195.64 ppm) and Sr content slightly enriched (av. 296.73 ppm) may be related to the K-bearing minerals. The high concentrations of Pb and Cu due to presence of meneghinite and

bayldonite minerals. Y is also enriched in these stream sediments with average (76.50 ppm), which is higher than that in UCC (21 ppm). Y presents in these stream sediments only within uranorthorite and zircon.

Table 1: Trace elements (ppm) analyses of the stream sediments, Wadi Abu Marw area.

Element/S.No	Cr	Co	Ni	Cu	Zn	Zr	Rb	Y	Ba	Pb	Sr	V	Nb
SM1	41	52	18	757	81	256	180	41	235	516	290	39	11
SM2	55	40	17	541	65	311	202	68	209	456	325	22	15
SM3	37	33	20	362	89	241	191	118	190	511	255	41	16
SM4	47	71	14	223	191	305	256	150	322	449	348	60	11
SM5	61	86	13	691	117	270	211	67	220	349	389	31	21
SM6	39	49	24	814	91	317	195	81	341	123	298	25	23
SM7	42	74	9	463	55	179	173	96	192	420	834	66	13
SM8	30	56	29	771	25	106	166	57	169	341	290	97	16
SM9	51	33	11	856	67	345	210	80	150	663	185	40	25
SM10	46	20	18	441	68	310	223	93	239	229	206	30	17
SM11	38	51	18	650	57	244	184	146	175	730	181	56	5
SM12	29	80	13	534	82	198	133	73	279	421	256	17	13
SM13	56	52	17	345	56	157	179	80	209	444	288	81	14
SM14	37	51	27	609	77	138	166	96	265	589	250	28	12
SM15	30	34	8	644	93	237	200	47	230	230	382	92	18
SM16	48	63	22	383	62	340	156	69	330	503	260	45	26
SM17	55	27	16	541	68	273	155	46	173	691	291	41	13
SM18	58	59	26	456	70	284	234	50	147	779	242	22	7
SM19	47	40	19	637	62	193	255	23	138	448	182	35	12
SM20	37	19	21	489	48	190	199	56	249	438	274	38	13
SM21	26	44	18	662	61	222	203	78	195	369	266	63	17
SM22	34	46	15	334	86	256	233	68	188	568	236	38	19
Min.	26	19	8	223	25	106	133	23	138	123	181	17	5
Max.	61	86	29	856	191	345	256	150	341	779	834	97	26
Av.	42.91	49.09	17.86	554.68	75.95	244.18	195.64	76.50	220.23	466.68	296.73	45.77	15.32
UCC	92	17.5	47	28	67	193	84	21	628	17	320	97	12

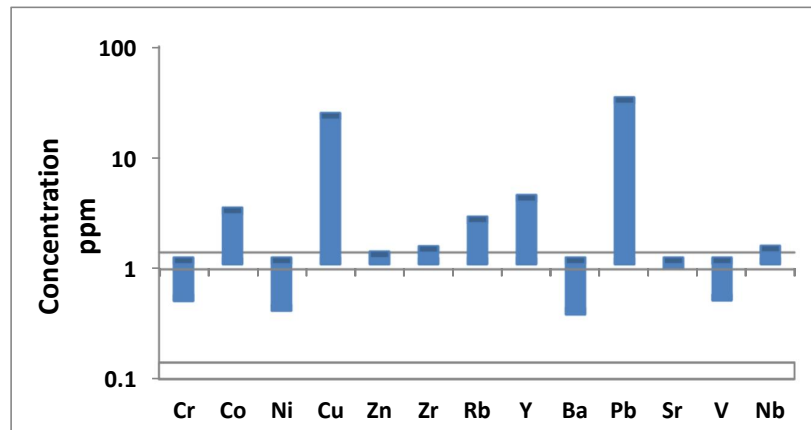


Fig. 13: Average of trace elements concentrations in stream sediments of Wadi Abu Marw compared with UCC.

Radioactivity

All the studied samples were radiometrically analyzed to determine their contents of eU, eTh, Ra (eU) (ppm) and K (%). The ratio eTh/eU was calculated as well as eU/ Ra (eU) ratio in order to test their radioactive equilibrium which would help to predict the U mobilization and the origin of mineralization if present. The radiometric measurements of the stream sediments samples are given in (Table-2). Under magmatic conditions, thorium is generally three times more abundant than uranium; i.e. the Th/U ratio is generally about 3-3.5 (chondritic ratio). The eTh/eU ratios are controlled by the redistribution of uranium that in turn is controlled by the epigenetic processes. The structural features play an important role in redistribution of uranium leading to depletion and/or enrichment.

The studied samples are characterized by low uranium and slightly high thorium contents with an average eU=3 ppm and an average eTh=11.59 ppm (Table-2). The binary relation between eU and eTh shows positive relation with reasonable correlation coefficient (r=0.38) (Fig. 14A). The ratio eTh/eU (av. =4.47) is relatively higher than the chondritic value (3-3.5) (Rogers and Adams, 1969) which is referred to the depletion of uranium in the studied samples. Uranium has low degree of correlation with potassium (Fig. 14B), this is attributed to leaching of uranium from stream sediments due to its great mobility. While thorium gave high moderate potassium correlation with potassium due to the high stability of thorium minerals (Fig. 14C).

The radioactive equilibrium/disequilibrium is considered as an essential part in the radiometric investigation of U-ore deposits and U-bearing rocks; it can be used as a tool for U exploration processes. In nature, the equilibrium state is controlled by different geologic processes such as weathering, alteration, groundwater, meteoric water, circulating fluids through fractures and fault planes. The equilibrium/disequilibrium state was discussed through calculation of the equilibrium factor (P) which is defined as: $P = eU/Ra$ (Hussein, 1978 and El Galy, 2003). The equilibrium state is reached, if the eU/Ra ratio is equal to unity. The obtained data in table (2) show that the studied samples (P-factor=1.4) indicate disequilibrium state which refer to slightly enrichment of uranium contents rather than Ra. The slightly enrichment of Th contents in the studied area is attributed to the presence of uranotorite and monazite minerals.

Table 2: Radioactivity measurements for the studied stream sediment samples

Sample No.	eU	eTh	Ra	K%	eTh/eU	eU/Ra
SM1	4	15	3	2.49	3.75	1.33
SM2	6	19	2	2.24	3.17	3.00
SM3	1	18	2	2.79	18.00	0.50
SM4	3	17	2	2.44	5.67	1.50
SM5	4	11	3	3.48	2.75	1.33
SM6	5	11	2	2.11	2.20	2.50
SM7	3	24	4	2.16	8.00	0.75
SM8	4	23	4	2.96	5.75	1.00
SM9	3	15	2	2.86	5.00	1.50
SM10	2	7	1	2.27	3.50	2.00
SM11	2	5	2	2.17	2.50	1.00
SM12	1	6	2	2.16	6.00	0.50
SM13	2	4	2	2.31	2.00	1.00
SM14	3	20	3	2.64	6.67	1.00
SM15	1	4	2	1.91	4.00	0.50
SM16	3	14	3	2.38	4.67	1.00
SM17	2	5	1	2.14	2.50	2.00
SM18	5	8	2	2.48	1.60	2.50
SM19	3	7	2	3.01	2.33	1.50
SM20	2	5	3	2.18	2.50	0.67
SM21	2	8	1	2.17	4.00	2.00
SM22	5	9	3	1.89	1.80	1.67
Min.	1	4	1	1.89	1.6	0.5
Max.	6	24	4	3.48	18	3
Av.	3	11.59	2.32	2.42	4.47	1.40

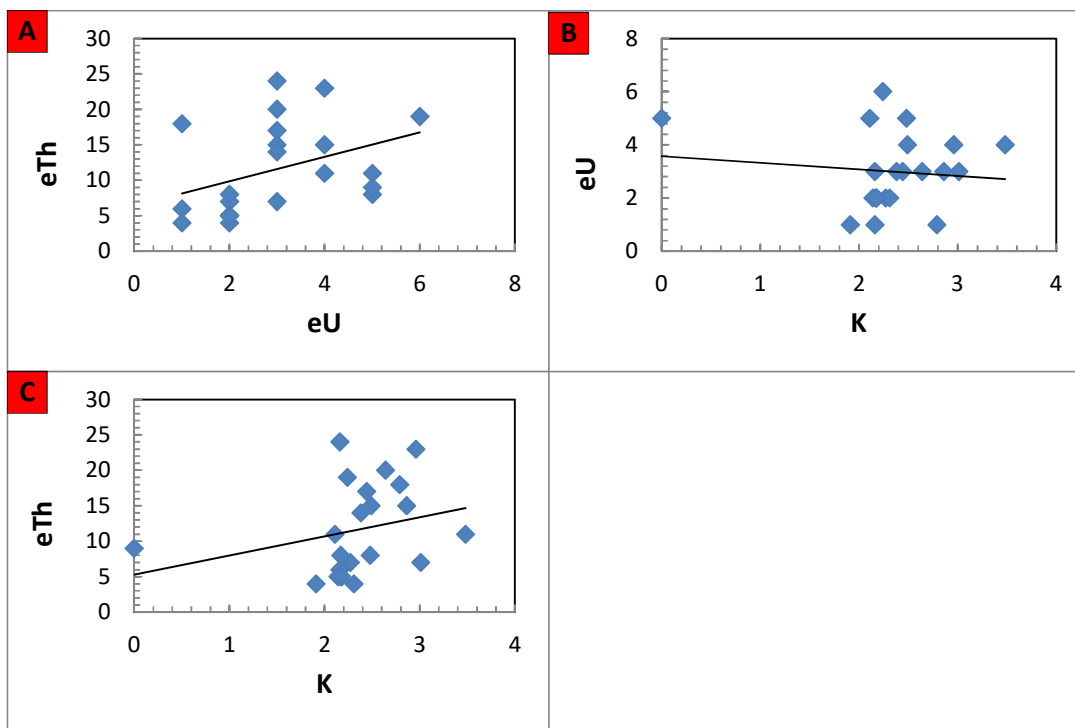


Fig. 14: A) eU-eTh, B) K-eU and C) K-eTh binary relations of the studied stream sediments.

Conclusion

The Abu Marw area is mainly covered by Late Proterozoic igneous and metamorphic rocks. The rock assemblages cropping out at Wadi Abu Marw area are; metagabbros, metavolcanics, older granites and younger granites.

The heavy minerals in the concerned stream sediments have been apparently derived from the weathering of the surrounding country rocks. The heavy minerals recognized microscopically are categorized to radioactive minerals (uranthorite), radioactive-bearing minerals (monazite and zircon) and non-radioactive minerals (magnetite, ilmenite, leucosene, titanite, jarosite, spessartine, rutile, fluorite, pyrite, apatite, stibiconite, wolframite, hübnerite, scheelite, cuprotungstite meneghinite, bayldonite, cassiterite and bismuth) as well as the green silicates.

The results of XRF analyses of twenty two samples from Wadi Abu Marw stream sediments revealed that these stream sediments are slightly enriched in Cu, Zn, Zr, Rb, Y, Sr and Nb and depleted in Cr, Ni, Ba and Pb comparing with the upper continental crust.

The stream sediments of Wadi Abu Marw area are characterized by low uranium and slightly high thorium contents which show a state of disequilibrium and depletion of U due to weathering processes affecting the studied area.

References

- Bea, F., 1996. Residence of REE, Y, Th and U in granites and crustal protolith; implications for the chemistry of crustal melt. *J. Petrol.*, 37: 521:552.
- Bea, F., M.D. Pereira, L.G. Corretage, and G.B. Fershtater, 1994. Differentiation of strongly peraluminous, perphosphorous granites: the Pedrobenards pluton, Central Spain. *Geochemica et Cosmochemica Acta*, 58: 2609-2627.
- Bishr, A.H.A., 2007. Factors controlling mineralizations of some shear zones in granites, South Sinai, Egypt. Ph. D. Thesis, Zagazig Univ., Faculty of Sci.
- Dardier, A.M., 1999. Morphology and geochemistry of zircon associated with uranium mineralization in Gattar granitic pluton, north Eastern Desert, Egypt. *Jour. Mineral. Soc. Egypt*, 11: 91-104.
- Deer, W.A., R.A. Howie, and J. Zussman, 1992. An introduction to the rock-forming minerals. (Second edition). ELBS with Longman. 696.

- El Aassy, I.E., H.M.Y. Sherif, and M.M. Gabr, 2006a. Genesis of uranium and thorium minerals on the scope of U-bearing zircon dissolution. Intern. Conf. Arab World (GAW8), Cairo Univ., Giza, Egypt, 317-324.
- El Afandy, A.H., 1994. Geology, petrology and radioactivity of the Basement rocks in Abu Marw SED-Egypt. Ph.D. Thesis, Fac. Sci., Assiut Univ., Aswan Branch.
- El Afandy, A.H., and G.B. El Shayib, 2020. Geology and distribution of radioelements as well as environmental impact at abu Marw younger granites, South Eastern Desert, Egypt. Egyptian journal of geology, 64: 279-295.
- El Afandy, A.H., A.A. Embaby, and M.A. El Harairey, 2015. Geology, geochemistry and radioactivity of granitoid rocks of abu Marw area, South Eastern Desert, Egypt. Nuclear Sciences Scientific Journal, 4: 61- 83.
- El-Galy, M.M., 2003. Review Article in Application of Equilibrium-Disequilibrium phenomena of the U-Th Decay series in Exploration for uranium ore Deposits. NMA.
- El-Mansi, M.M., A.M. Dardier, and I.M. Abdel Ghani, 2004. Crystal habit and chemistry of zircon as a guide for uranium redistribution in Gabal Ria El-Garrah area, Eastern Desert, Egypt. Delta Jour. Of Sci., 28: 19- 30.
- El-Nahas, H.A., 2006. Distribution of nuclear minerals in G. Hamra environs, Southern Sinai, Egypt. Ph.D. Thesis, Fac. Sci., Minufiya Uni., Egypt., 159.
- Elsner, H., 2010. Heavy minerals of economic importance. Assessment manual, Faculty of Geosciences of the University of Hannover: 218p. 31 Fig. 125 Tab.
- Fayziev, A.R., 1990. Yttrium in fluorite from endogenous shows in USSR. Translated from Geokhimiya, 7:1037-1042.
- Finch, R.J., and J.M. Hanchar, 2003. Structure and chemistry of zircon and zircon-group minerals. Reviews in mineralogy and chemistry, 53: 1-25.
- Förster, H.J., 2006. Composition and origin of intermediate solid solutions in the system thorite-xenotime-zircon-coffinite. Lithos., 88: 35–55.
- Fronde, C., 1958. Systematic mineralogy of uranium and thorium. U. S. Geol. Survey Bull. 1064: 160-170.
- Gbaruko, B. C., and J.C. Igwe, 2007. Tungsten: Occurrence, Chemistry, Environmental and Health Exposure Issues. Global Journal of Environmental Research. 1 (1): 27 - 32.
- Goldmann, S., F. Melcher, H. Gäbler, S. Dewaele, F. DE Clercq, and P. Mucchez, 2013. Mineralogy and Trace Element Chemistry of Ferberite/Reinite from Tungsten Deposits in Central Rwanda. Minerals, 3:121-144; Doi: 10.3390/min3020121
- Harzanagh, A.A., S.L. Ergun, and E. Gulcan, 2017. Beneficiation of oxide ores using dense medium cyclones. A simulation study Physicochem. Probl. Miner. Process. 53(1): 379–393.
- Hinton, R.W. and B.A. Paterson, 1994. Crystallization history of granitic magma: evidences from trace elements zoning. Mineral. Mag., 58A, P. 416:417.
- Horsnail, R.F., 1979. The geology of tungsten. In: Proceedings of the First Tungsten Symposium. Stockholm, September 5-7, Mining Journal Books Limited, 18–31.
- Hussein A.H., 1978. Lecture Course in Nuclear Geology, P.101, NMA, Egypt.
- Khazback, A.E. and M.F. Raslan, 1995. Potentialities of physical up-grading of Gebel Gattar uranium ore, Eastern Desert, Egypt. Al-Azhar Bull. Sci., 5: 1-7.
- Martins, J.I., 2014. Leaching Systems of Wolframite and Scheelite: A Thermodynamic Approach, Mineral Processing and Extractive Metallurgy Review: DOI:10.1080/08827508.2012.757095. Materials. J. Mater Sci, 54: 83–107.
- Mcclenaghan, M.B., M.A. Parkhill, A.A. Seaman, A.G. Pronk, M. Mccurdy, D.J. Kontak, 2014. Overview of tungsten indicator minerals scheelite and wolframite with examples from the Sisson W-Mo deposit, Canada. Application of Indicator Mineral Methods to Mineral Exploration, Short Course SC07 26th International Applied Geochemistry Symposium. 59-67.
- Mohamed, E.H., 1987. Mineralogical studies for some Quaternary sediments in northern Sinai. M. Sc. Thesis, Ismailia Univ.
- Mohamed, S.S.M., 1998. radioactivity and mineralogic studies on wadi Abu Dabbab alluvial deposits, Central Eastern Desert, Egypt. M. Sc. Thesis, Fac. of Sci., Ain Shams Univ. 204.

- Omran, A.A., and O.K. Dessouky, 2016. Ra's Abdah of the north Eastern Desert of Egypt: the role of granitic dykes in the formation of radioactive mineralization, evidenced by zircon morphology and chemistry. *Acta Geochim.* 354: 368–380.
- Pupin, J.P., B. Bunin, M. Tessier, and G. Turco, 1978. Role de l'eau sules caracteres morphologiques, et la cristallisation du zircon dans les granitoides. *Bull. Soc. Geo. Fr.*, 20: 721-725.
- Read, F.R.S., 1970. *Rutley's elements of mineralogy*. London, Thomas Murby Co., 560.
- Rogers, J.J.W. and J.A.S. Adams, 1969: Uranium and thorium. In: Wedepohl. K.H. (ed.), *Handbook of geochemistry*, New York, Springer Verlag, 4, 92-B-1 to 92-C-10.
- Rollinson, H.R., 1993. "Using geochemical data: evaluation presentation and interpretation", Longman Scientific and technical Pree, Jhon Willy and Sonic. New York, USA. 398.
- Rudnick, R. L., and S. Gao, 2003. Composition of the continental crust. In: Holland, H.D., Turekian, K.K. (Eds.), *Treat. Geochem*, 3: 1-64.
- Sengupta, A.K., A.S. Aragopal, S.S. Jagdish Lal, G.M. Rao, and K. Satyanarayana, 1987. The recovery of tungsten mineral from granite rock – a non-conventional approach. *Próba niekonwencjonalnego wydzielenia mineralów wolframu ze skal granitowych (in Polish)*. *Physicochem. Probl. Miner. Process.*, 19(1): 195–204.
- Sherif, H.M.Y., 1998. *Geology and uranium potentiality of Wadi Seih area, southwest Sinai, Egypt*. Ph.D. Thesis, Cairo Univ. Geza, Egypt. 229.
- Srivastava, R.R., J. Lee, M. Bae, and R.V. Kuma, 2019. Reclamation of tungsten from carbide scraps and spent Materials. *J. Mater Sci.*, 54: 83–107.